ACS Sustainable Chemistry & Engineering

pubs.acs.org/journal/ascecg

Research Article

High-Performance Sensors Based on Chinese Ink and Water-Based Glue for Detection of Strain, Temperature, and Humidity

Banghan Liu, Youquan Zhou, Linhong Chen, Yue Feng, and Mingxian Liu*

Cite This: *ACS Sustainable Chem. Eng.* 2022, 10, 1847−1856

Read Online

ACCESS | Metrics & More | Article Recommendations | Supporting Information

ABSTRACT: Flexible sensors with high sensitivity and reproducibility have critical applications in various industrial fields. However, current sensors have not yet been able to respond to diverse signal changes in the environment due to their poor stability, weak conductivity, high cost, and time-consuming integration process. Herein, we used dip-coating technology to prepare multifunctional rubber flexible sensors which were based on the Chinese ink carbon nanoparticle (ICN) and water-based glue. The prepared flexible sensors have the ability to sensitively detect temperature, humidity, and strain signals. The conductive ICN can well adhere on the elastic substrate (natural rubber latex glove), which gives the flexible sensors excellent structural stability even after 500 cycles. The strain response and recovery time of the flexible sensors are 132.8 and 133.8 ms, respectively. The flexible sensors can sensitively detect tiny pressure, human body movements, pronunciation, and human facial expression. Moreover, the prepared high-performance flexible sensors can also be used as temperature and humidity sensors, which displayed a good linear relationship between resistance change and the external signals. This work developed a simple, green, high-efficiency, and low-cost flexible sensors, which shows promising potential in wearable electronic devices for detection of strain, humidity, and temperature.

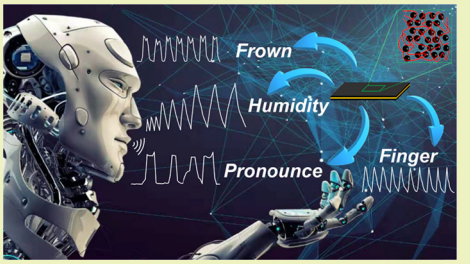

KEYWORDS: *Chinese ink, PVA glue, multifunctional, sensor, high stability*

INTRODUCTION

Flexible sensors are bendable or foldable devices that can convert external stimuli such as deformation, temperature, humidity, pressure, and force into electrical signal outputs.[1] In recent years, with the rapid development of intelligent technology, flexible sensors are widely used in various fields, such as temperature detection,[2−4] humidity monitoring,[5−7] human motion detection,[8−12] generating electricity,[13,14] and so on. Flexible sensors are favored because of their recoverability, light weight, and high flexibility.[15−20] However, the complex preparation process, low stability, poor conductivity, high cost, and other shortcomings limit the practical application of flexible sensors. Therefore, it is urgent to propose a flexible sensor with simple preparation, low cost, and good stability.

Currently, the materials used in the preparation of flexible sensors mainly include hydrogel,[21−23] fiber,[24−26] and rubber.[27−29] Compared with hydrogels and fibers, rubber materials have the advantages of high elasticity, abrasive resistance, and modulus. Therefore, rubber matrix materials are more suitable for preparing flexible sensors. For all kinds of flexible sensors, the conductive network is the core. There are various methods to design the conductive network, such as surface penetration technology,[8] continuous wet-spinning,[9] and dip-coating technology. Dip-coating technology is favored because of its simple operation and short preparation processes time. Inspired by this, this research intended to use dip-coating technology to achieve rapid preparation of flexible sensors.

Carbon material is a good conductor for preparing flexible sensors, such as carbon black,[30,31] carbon nanotubes,[32−34] graphene,[35,36] and so forth. However, these materials used to prepare flexible sensors usually require long preparation time and high cost. Chinese ink, as a mixture of soot and animal glue, has been widely used in calligraphy and brush painting in East Asia for thousands of years.[37] Generally, the carbon used was either soot made by burning wood (usually pinewood) or lampblack made by burning oil at a wick, while the animal glue binder was manufactured mostly from the hides of mammals to yield a strong collagen-based glue. The ink is mainly composed of carbon nanoparticles, which possess many advantages such as intrinsic color of black, good water-dispersion stability, strong adhesion to material surfaces, proper fluidity, and outstanding photothermal performance.[38,39] Our previous work verified that Chinese ink carbon nanoparticle (ICN)-coated melamine foam has expressed excellent Joule heating and photothermal effect, which show promising application in strain sensor and seawater desalination.[40] Jiang et al. used a writing ink made from graphene nanosheet as a conductive

Received: October 29, 2021
Revised: January 12, 2022
Published: January 27, 2022

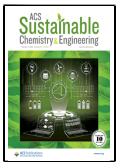

https://doi.org/10.1021/acssuschemeng.1c07174
ACS Sustainable Chem. Eng. 2022, 10, 1847−1856

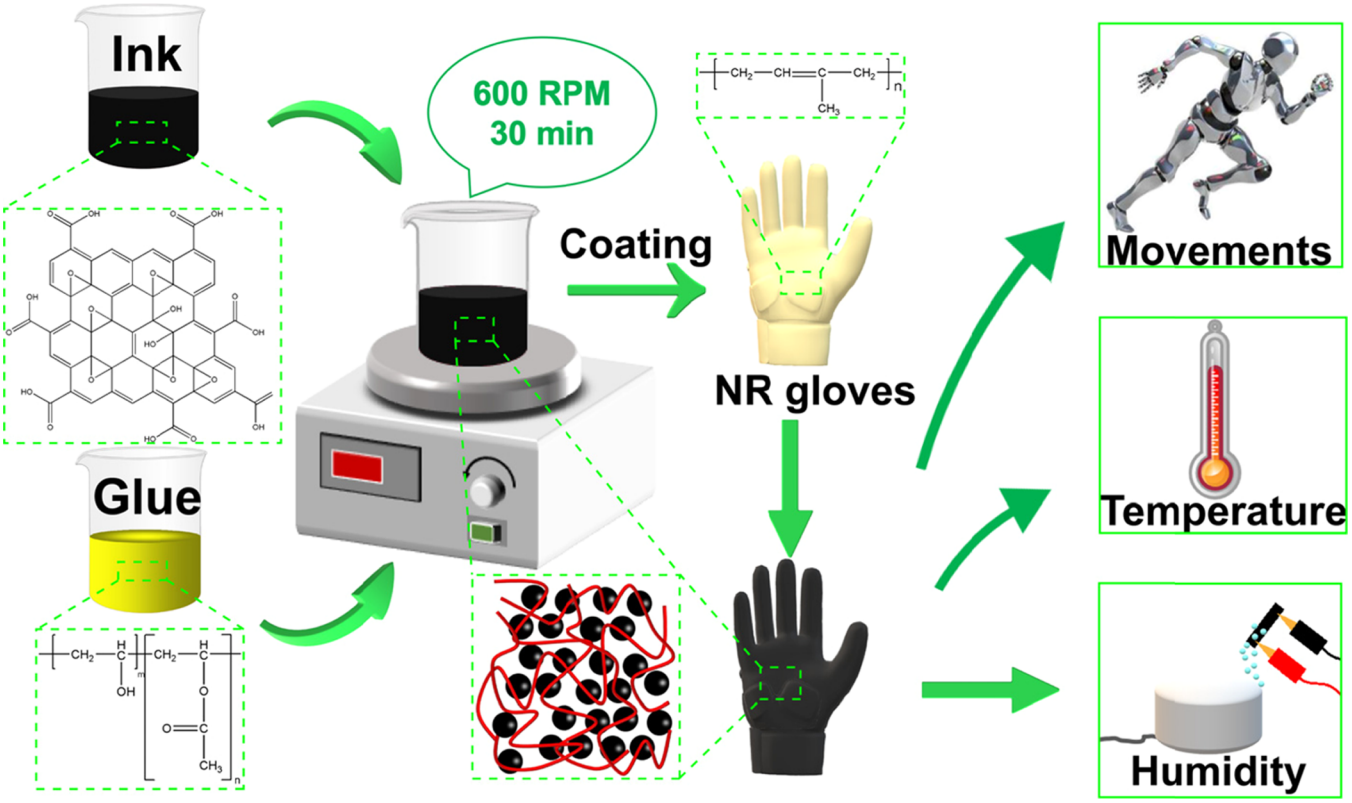

Figure 1. Preparation process of the Ink/Glue/NR sensor: Chinese ink was mixed with PVA glue in different mass ratios (ink: glue = 0.5:1, 1:1, 1.5:1, 2:1, and 3:1) and stirred magnetically at 600 rpm for 30 min. Then, the ink/glue mixture was evenly coated on the surface of the NR latex gloves and dried at 60 °C for at least 24 h. During the drying process, the PVA glue gradually solidifies, and the ICN can be adhered to the surface of the gloves. Finally, the gloves was cut to the desired rectangular shape with a knife to prepare the Ink/Glue/NR sensor. The application field of the Ink/Glue/NR sensor: human movement detection, temperature monitoring, and humidity monitoring.

component to prepare a flexible potentiometric sensor.[41] In addition, multifunctional sensors that combine multiple functions into one sensor have become the research hotspots recently.[42,43] Integrating different monitoring functions on one flexible sensor can measure several parameters at the same time, and the collected information is concentrated and easy to process. For instance, Yao et al. used surface penetration technology by immersing natural rubber (NR) in carbon black suspension to fabricate strain sensors that can detect weight, sound pressure, and dripping of tiny droplets.[8] Bi et al. reported silver nanoparticle-modified polyimide for the detection of multiple artificial skin sensing.[44] These works provide clues for us to develop multifunctional sensors, which may detect more external stimuli with one device.

In this work, a multifunctional sensor that can detect strain, temperature, and humidity was prepared using NR as the flexile matrix and using ICN as the conductive network. Polyvinyl alcohol (PVA) glue was used to increase the interfacial adhesion between the ink and the rubber matrix (Figure 1) because the molecular chain of PVA contains a large number of hydroxyl groups which can form hydrogen bonds with the surface of carbon materials. During the drying process, the glue gradually solidifies, so that the ICN is well attached to the NR matrix. The microstructure and the sensor performance of a series of flexible sensors were investigated in detail. This simple, green, high-efficiency, and low-cost flexible sensor can be applied to the detection of temperature, humidity, and human movements, which may find great potential in wearable devices and artificial intelligence. However, when these three factors are changed at the same time, this flexible sensor does not yet recognize their individual contribution.

RESULTS AND DISCUSSION

Characterization of Chinese Ink. ICN derived from Chinese ink have a chemical composition and microstructure similar to carbon black particles, which exhibit excellent electrical conductivity. A series of characterizations for the ICN were conducted. Figure S1A shows the appearance of the ink. The Tyndall effect of the diluted ink was confirmed, as a light beam can be observed upon irradiation of laser (Figure S1B). This indicated that the particle size of the ink is in nanoscale. The microstructure of ICN was then characterized by scanning electron microscopy (SEM) and transmission electron microscopy (TEM) (Figure S1C and 1D). It can be observed that ICN exists in the form of small spherical aggregates composed of amorphous flakes, with the size ranging from 20 to 60 nm. The X-ray diffraction (XRD) pattern of the dried ICN in Figure S1E shows a broad peak at about 25°, which is attributed to the crystal plane (002) of carbon. This typical characteristic is consistent with graphite carbon materials.[45] The Raman spectrum of the ICN (Figure S1F) shows the D-band (1343 cm^{-1}) and G-band (1587 cm^{-1}), which indicates that Chinese ink contains amorphous carbon and graphene sheet-like structures.[46] UV−vis analysis of diluted ink was then conducted (Figure S1G), and the result suggested that the absorption peak at 255 nm is assigned to the electronic conjugation in graphite.[47] The particle size distribution of ICN is shown in Figure S1H. It can be seen

https://doi.org/10.1021/acssuschemeng.1c07174
ACS Sustainable Chem. Eng. 2022, 10, 1847−1856

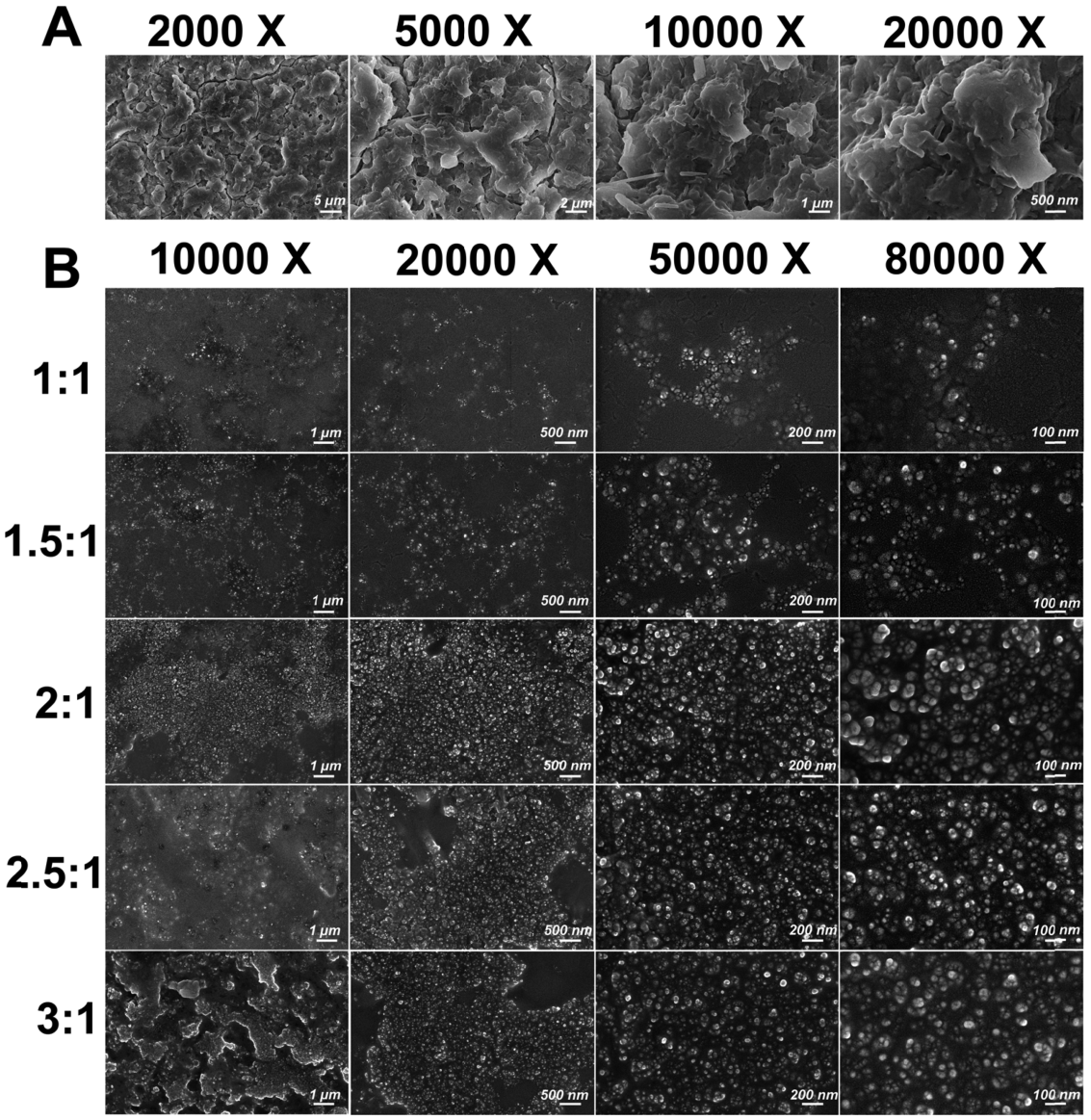

Figure 2. SEM images of the surfaces of NR (A) and different ink/glue-coated NR multifunctional sensors (B).

that the ICNs display a relatively narrow size distribution from 198.0 to 356.2 nm. The average size of ICN is 167.5 nm, while the zeta potential of ICN is −25.8 mV. The survey and the high-resolution spectra of XPS of nitrogen and oxygen element (Figure S2) suggest that the components of ICN are carbon and oxygen. C 1s and O 1s of the ICN appear at 284.5 and 533.2 eV, respectively. Carbon and oxygen contents in ICN are 84.3 and 15.7%, respectively.

Characterization of Ink/Glue Composites. The surface structures of the Ink/Glue composites and raw NR were observed using an SEM machine (Figure 2). It can be clearly seen that the surface of the NR exhibited a lamellar structure with a moderate roughness. When the Ink/Glue composites were coated on the rubber surface, the lamellar structure cannot be observed in the SEM images, indicating that the Ink/Glue composite layer can cover the rubber surface well. After the Ink/Glue composites were introduced on the rubber surface, a porous structure was found. This phenomenon can be attributed to the non-uniform volatilization of water in the ink and glue mixture, which leads to the phase separation. As the mass ratios of ink:glue increases, the number of pore structures becomes higher. The SEM images at 80,000X show that the ICN embedded in PVA glue is uniformly dispersed in the rubber surfaces, and the morphology of the ICN is similar to the initial sphere-like morphology, suggesting that the ICN shows no structural change during the coating and curing process.

The Fourier transform infrared spectroscopy (FTIR) spectrum of the Ink/Glue composites was then determined. As shown in Figure 3A, the PVA glue exhibited typical absorption peaks around 3300, 2850−3000, 1750−1735, 1141, and 1150−1085 cm^{-1}, which are assigned to O−H, C−H, C═O, C−O, and C−O−C groups, respectively.[48] The ink and glue composites showed the IR absorption peak of both PVA and ink, and the IR peaks of the PVA were partly shielded by the ICN. It is supposed that the compatibility between PVA glue and the ICN is good because they have hydrogen bonding interactions between hydroxyl groups of PVA and the oxygen-containing groups of the ICN. The XRD results of Ink/Glue composites are shown in Figure 3B. Basically, XRD profiles of Ink/Glue composites exhibited the characteristic peaks of both PVA (2θ = 19.5°, assignment of strong intermolecular and

https://doi.org/10.1021/acssuschemeng.1c07174
ACS Sustainable Chem. Eng. 2022, 10, 1847−1856

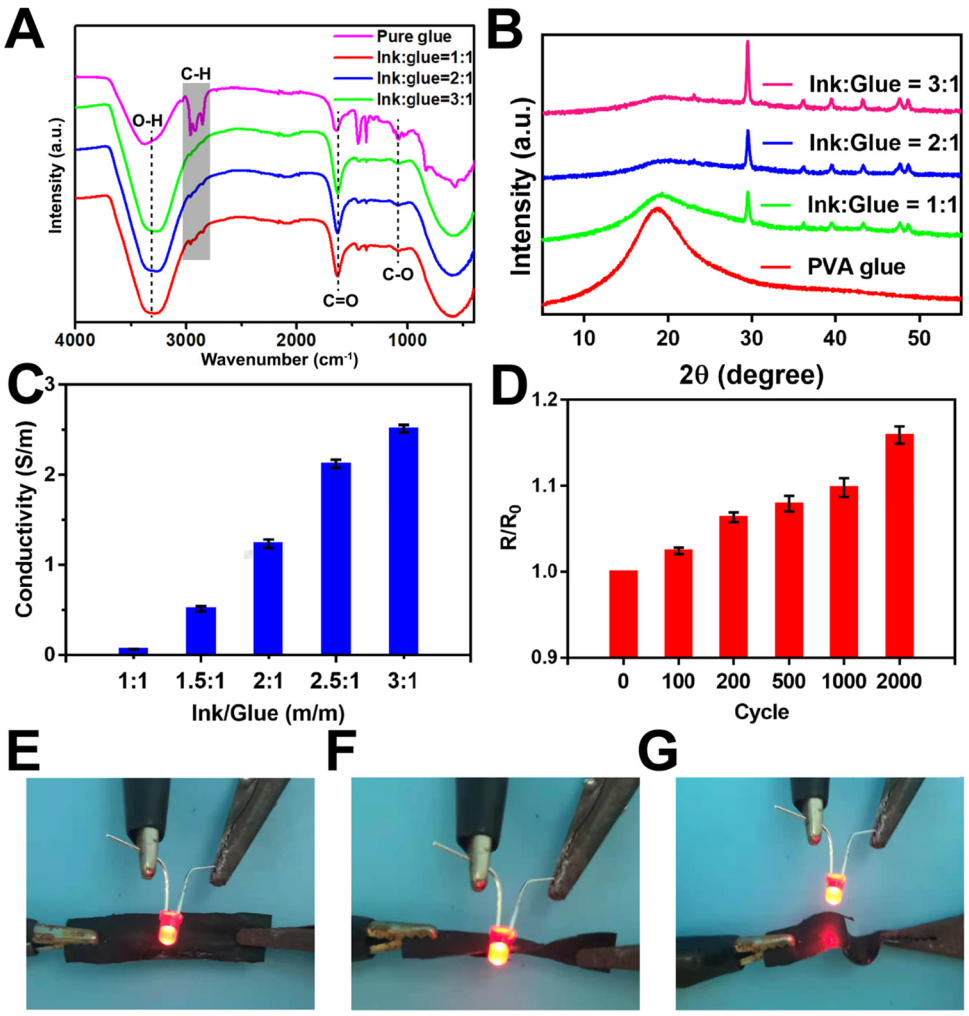

Figure 3. (A) FTIR of Ink/Glue composites with different mass ratios. (B) XRD pattern of PVA glue and Ink/Glue composites with different mass ratios. (C) Conductivity comparison of Ink/Glue composites. (D) Change of electrical conductivity of Ink/Glue (2:1) composites after different stretch−recycle cycles. Photographs showing the stable illumination of the LED bulb when the Ink/Glue (2:1) composites were (E) straight, (F) twisted, and (G) bent.

intramolecular hydrogen bonding of PVA) and ICN (2θ = 29.0°, 002 crystal plane).[49,50] The (002) crystal plane of ICN shifts to a high diffraction angle because there are hydrogen bonding interactions between PVA and ICN. Figure 3C shows the electrical conductivity of the Ink/Glue composites with different Ink/Glue mass ratios. When the ratio of ink and glue is 1:1, the conductivity of the Ink/Glue composite is 0.064 s/m. The conductivity of the composite increases rapidly when the mass ratios increase to 3:1, and its conductivity reaches to 2.520 s/m. This suggested the good conductivity of the ICN and the good interfacial interactions in the composites. The weight ratio of the Ink: Glue of 2:1 was used in following testing. As shown in Figure 3D, the Ink/Glue composites were used in stretch−recovery cycle (each strain is about 50%) to detect the change of conductivity. The results show that the composite can maintain good conductivity even after being subjected to multiple stretch−recovery cycles (the resistance only increases to 115.8% of the initial value after 2000 cycles), indicating that the sensor has the ability to be used for a long time. When the Ink/Glue composites were changed at different shapes, such as twisted (Figure 3F) and bent (Figure 3G), the brightness of the LED bulb is consistent with the initial state (Figure 3E) of the Ink/Glue composites. This illustrated that the Ink/Glue composite is a conductor with excellent flexibility and stability.

Ink/Glue composites have high stability to withstand diverse harsh environments. As shown in Figure S3A, we put the composites in 1 mol/L HCl, 1 mol/L NaOH, and 0.01 mol/L phosphate buffered saline (PBS) for 30 days. After 30 days, the Ink/Glue composites were taken out. It was found that the Ink/Glue composites still adhered well to the NR, which proved that the Ink/Glue composites have excellent adhesion and resistance to various environments. In addition, the Ink/Glue composites can remain stable in 0.01 mol/L PBS, which provides a potential application for wearable electronic devices. The conductivity of the sensor decreases very little after being immersed in different environments for 30 days (Figure S3C), which can preliminarily indicate that the sensor can remain stable in a common environment.

Performance of the Ink/Glue/NR Sensor. Ink/Glue composites with a mass ratio of ink: glue of 2:1 were selected as strain sensors in virtue of their comprehensive properties. When the mass ratio of ink: glue is 3:1, the conductivity is indeed the largest (Figure 3B), but the sensing performance is worse than 2:1. The strain sensitivity of the sensors was first studied. Figure 4A,B show the changes in the relative resistance

https://doi.org/10.1021/acssuschemeng.1c07174
ACS Sustainable Chem. Eng. 2022, 10, 1847−1856

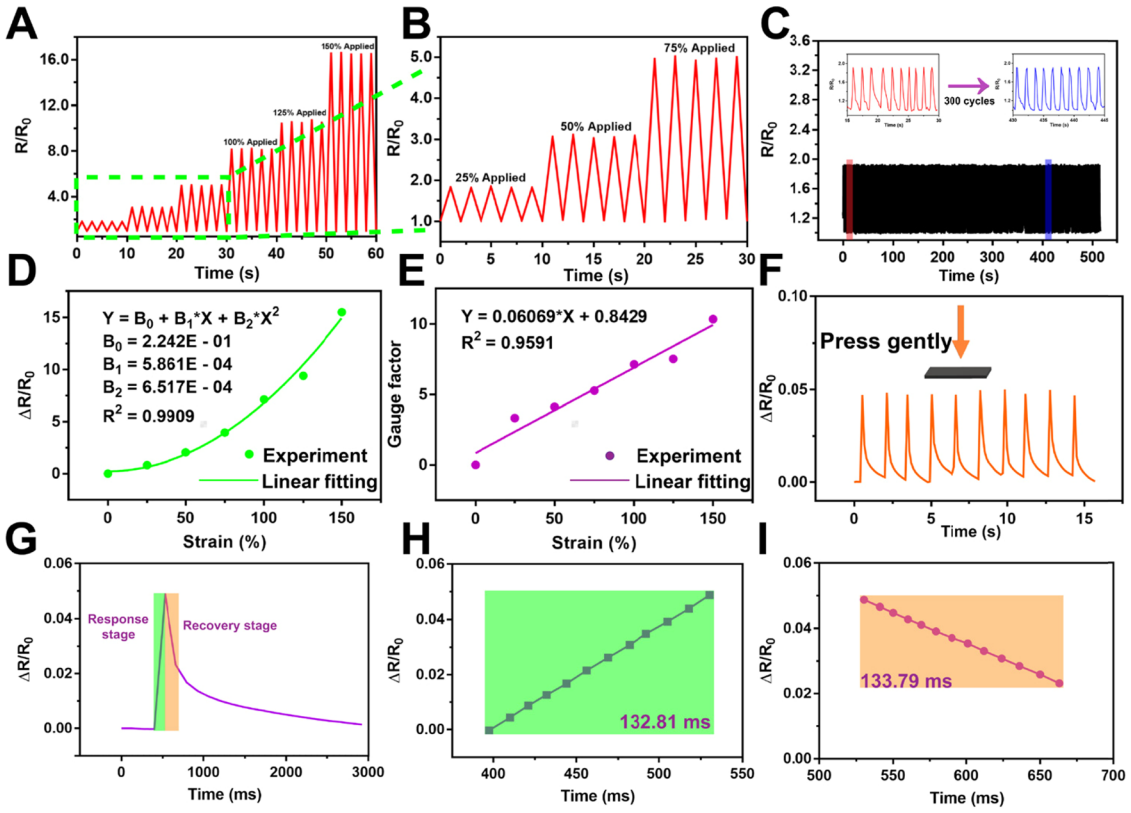

Figure 4. (A) Dynamic stretch−release cycle response of the sensor for various strains from 25 to 150%. (B) Stretch−release cycles for 25, 50, and 75%. (C) Cycle stability test of the sensor during bending and extending stretching and releasing. (D) Response of the resistance of the sensor to strain. (E) Gauge factor of the sensor. (F) Response of the sensor to strain caused by gently pressing. (G) Instant response of the Ink/Glue composite, which shows response time and recovery time of 132.81 (H) and 133.79 (I) ms, respectively.

R/R_0 of the strain sensors in six tensile release cycles of 25, 50, 75, 100, 125, and 150%. It can be clearly seen that in each stretch−release cycle under large strain, the relative resistance R/R_0 of the sensor is basically the same, which shows that the strain sensor has excellent stability and high elasticity under a maximum strain of 150%. Furthermore, it is worth mentioning that the strain sensor could still hold quite stable output signals even after 500 cycles at a strain of hand stretch (Figure 4C), demonstrating excellent stability and repeatability. As shown in Figure 4D,E, the resistance changes $\Delta R/R_0$ as a function of strain (ε) of the sensor were plotted, and the corresponding gauge factor (GF) (GF = $(\Delta R/R_0)/\varepsilon$) was calculated to evaluate the electrical sensitivity of the strain sensor. What is interesting is that the relationship between the sensor's resistance change and strain fits a quadratic function relationship (Figure 4D).[51,52] At the same time, it can be found from the calculation formula of GF that when the relationship between the sensor's resistance changes and strain fits the quadratic function relationship, GF and strain become proportional (Figure 4E). Therefore, Chinese ink is superior to carbon black, graphene, and carbon nanotubes in terms of sensitivity, response time, linearity, and cost of fabrication (Table S1).

The strain sensor can also capture the deformation caused by pressing gently and gave regular response signals accurately (Figure 4F). The response and recovery performances of the strain sensors were tested by quickly stretching and releasing (Figure 4G). The strain sensors exhibited the characteristic of same response and recovery time, indicating the good repeatability and structural stability of the sensor. The response or recovery time of the sensor is 132.8 (Figure 4H) and 133.8 (Figure 4I) ms, respectively. This suggests that the sensor has a quick response ability, which can find application in practical strain detection.

Applications in Pressure Monitoring. One of the applications of Ink/Glue/NR sensors is pressure detection. At first, the pressure sensor was fixed on the table with tape and connected to the electrometer with electric wires. Then, the tester pressed the sensor with different fingers, and the resistance change of the sensor was carefully recorded. When the pressing fingers were different, the resistance change of the pressure sensor was also obviously different (Figure S4).

The sensor was attached to the microphone of a mobile phone (Figure S5A), and a slight change in pressure was achieved by changing the sound volume of the mobile phone. As shown in Figure S5B−D, when the same bell sound is played with the mobile phone, the resistance of the sensor changes. The pressure sensor can accurately detect changes in decibels. Different decibels produce response signals corresponding to different intensities. The greater the decibel was, the greater was the value of $\Delta R_{max}/R_0$. The response signal at the same decibel has excellent stability and repeatability. The results show that the pressure generated by the sound can be accurately detected by the pressure sensor.

The pressure sensor was then attached onto a steel ruler for demonstrating its ability to detect the physical vibrations (Figure S6A,B). When the ruler vibrated, the first vibration amplitude was the largest, the vibration amplitude of the steel ruler gradually decreased due to the friction of the air, and finally, the vibration of the ruler reached a standstill. As shown

https://doi.org/10.1021/acssuschemeng.1c07174
ACS Sustainable Chem. Eng. 2022, 10, 1847−1856

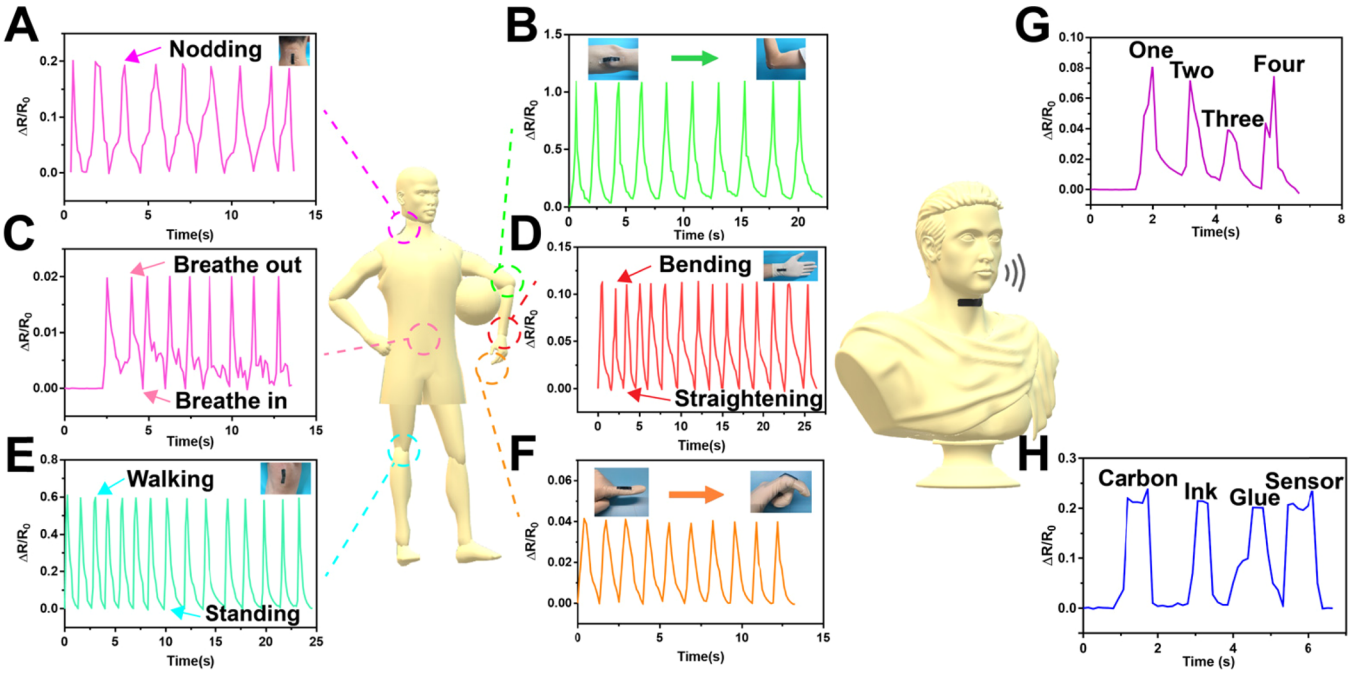

Figure 5. Detection of human movements: (A) nodding; (B) elbow movements; (C) breathing; (D) wrist movements; (E) standing and walking; (F) finger movements; and (G,H) detection of pronunciation.

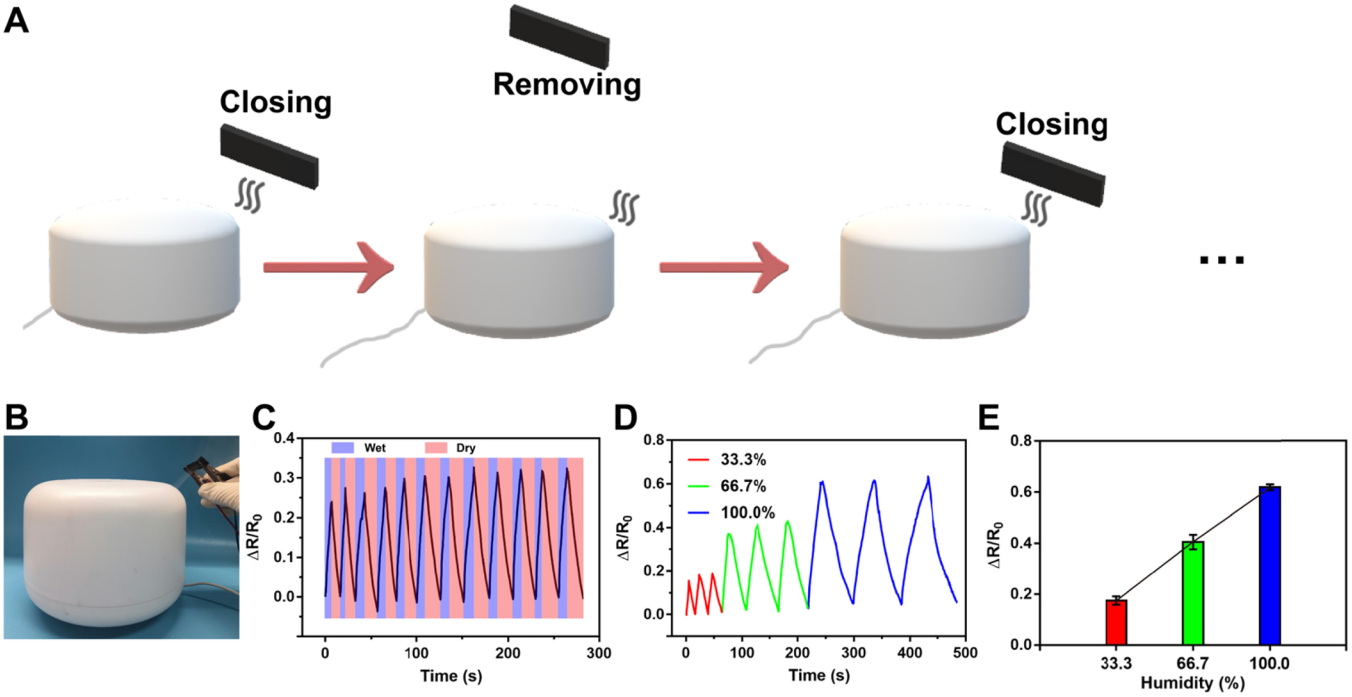

Figure 6. Schematic and photographs showing the process of humidity detection (A,B) and the recorded current resistance signals when closing and removing the humidity sensor to the humidifier (C). Relationships show current patterns in the process of changing humidifier's power (D) and $\Delta R_{max}/R_0$ (E).

in Figure S6C, the pressure sensor exhibited a superb and stable response to damped vibration of the ruler. Figure S6D shows the enlarged view of the green dotted box in Figure S6C, which demonstrates the gradual change in resistance. These results suggest that the pressure sensor can be applied in detection of various vibrations in human daily life.

Applications in Detection of Human Movements. The Ink/Glue composites were coated by dip-coating technology on the outer surface of the NR, while the inner surface of the Ink/Glue/NR sensor was insulated. In order to detect human movements, the inner surface of the Ink/Glue/NR sensor directly contacts the tester's body. Due to its excellent performance, the strain sensor can detect different human movements, from large (joint movements) to tiny (breathe) scale. Figure 5A shows that the bending of the cervical vertebra can be detected by attaching the strain sensor to the cervical

https://doi.org/10.1021/acssuschemeng.1c07174
ACS Sustainable Chem. Eng. 2022, 10, 1847−1856

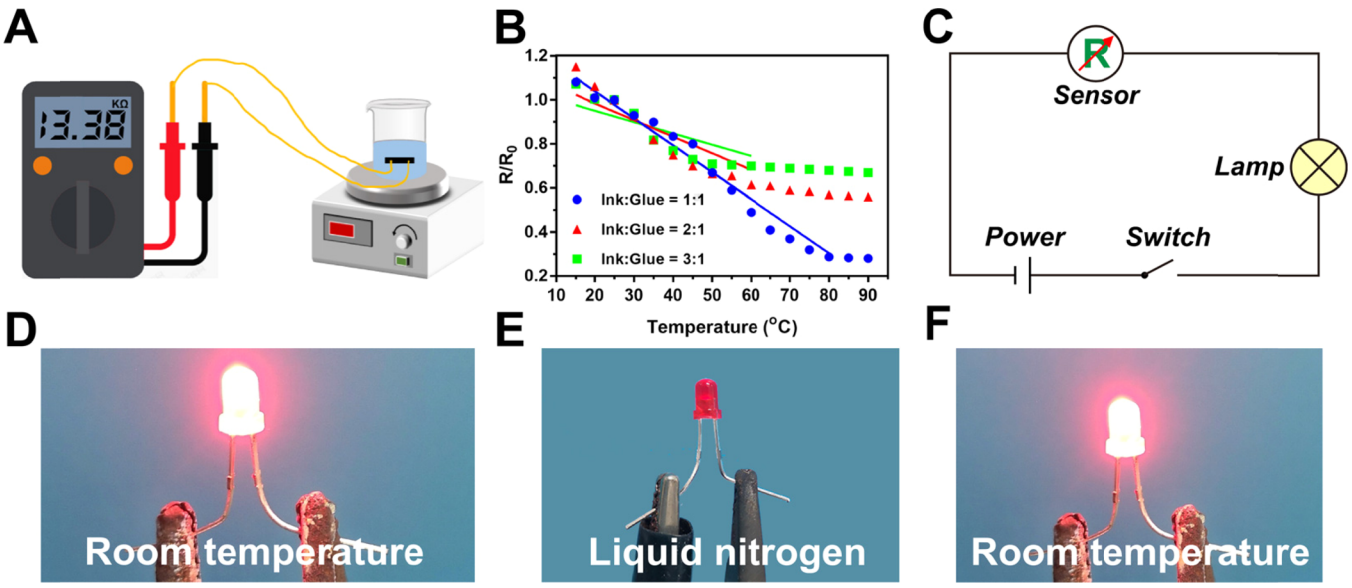

Figure 7. (A) Schematic diagram of the Ink/Glue/NR sensor used for temperature detection; (B) resistance changes of the sensor in relation to temperature; (C) circuit diagram of the LED bulb in series with the temperature sensor; (D) brightness of an LED bulb when the sensor is placed at room temperature; (E) brightness of the LED bulb when the temperature sensor is placed in liquid nitrogen; and (F) brightness of an LED bulb when the sensor is removed from the liquid nitrogen and returned to room temperature.

vertebra. The value of $\Delta R/R_0$ increased rapidly with increasing bending of the cervical vertebra and returned to the original values when the cervical vertebra was straightened. Repeated bending and straightening of the cervical vertebra at the same angle produced regular and periodic steady sensing signals. Figure 5B,D,E,F also shows that the bending of the elbow, wrist, knee, and finger joints can be sensitively detected by attaching the strain sensor to the elbow, wrist, knee, and finger.

The strain sensor can also be used to detect tiny human movements effectively. As shown in Figure 5C, signals from a volunteer breathing through his belly can be detected. Besides, speech recognition can be achieved by attaching the sensor to the throat. Figure 5G,H shows the strain sensor response signals when the tester said different words such as "one," "two," "three," "four," "carbon," "ink," "glue," and "sensor" and made a swallowing motion. When the tester says different words, the vocal cord vibrations corresponding to the different words are different, which leads to the change of output signals corresponding to the strain of the sensor. Moreover, the strain sensor can also be applied to detect small changes in facial expressions. Figure S7 shows the signal response of the strain sensor when the tester frowns, smiles, and winks. These results show that the sensor provides potential applications for human movement and human health monitoring.

Applications in Humidity Monitoring. Another application for prepared Ink/Glue/NR sensors is to detect changes in ambient humidity. Here, a humidifier (Y600, Yutu, China) was used to simulate the change of environmental humidity. The humidity around the sensor can be changed by moving the sensor close to the humidifier and away from the humidifier (Figure 6A,B). As shown in Figure 6C, when the humidity around the sensor increases, the resistance increases, and when the sensor is far away from the humidifier, the resistance returns to the original resistance. This phenomenon can be attributed to when the humidity increases, water molecules in the air enter the conductive network of the sensor, resulting in an increase in sensor resistance. While the environmental humidity decreases, the water molecules are removed from the conductive network, the conductive network recovers, and the resistance decreases. When the power of the humidifier changes, the $\Delta R_{max}/R_0$ of the sensor also presents different values. The humidity corresponding to the maximum humidification power of the humidifier is defined as 100%, and the change of environmental humidity is simulated and adjusted by changing the power of the humidifier. It can be seen that when the ambient humidity increases proportionally, the $\Delta R_{max}/R_0$ of the sensor also increases proportionally (Figure 6D,E). The humidity detection ability of the sensor can be attributed to the change of the reversible resistance when the water steam enters and escapes the conductive network of ICN.

Applications in Temperature Monitoring. Interestingly, the conductive Ink/Glue composites proposed in this work exhibit high stability in temperature monitoring. As the schematic given in Figure 7A shows, a 200 mL beaker was filled with 180 mL of dimethyl silicone oil, and a thermometer was placed in the beaker. The temperature sensor was attached to the outer wall of the beaker with tape, and the temperature sensor was connected to the multimeter with electric wires. The temperature around the sensor increased by heating the beaker. As shown in Figure 7B, as the temperature increases in the temperature range of 10−90 °C, the resistance of the sensor gradually decreases. Similar to the mechanism of humidity sensing, when the ambient temperature increases, the conductive network shrinks due to heat, and the resistance becomes smaller. While the ambient temperature drops, the movement of the conductive particles is restricted, so the resistance increases. An approximate linear relationship (R^2 = 0.9444) of the Ink/Glue with a 1:1 ratio was found in the temperature range of 15−80 °C. Therefore, the resistance of the sensor is inversely proportional to the environment temperature. Therefore, the sensor can be used to display of danger signals to prevent burning or scalding. The temperature resistance response of the sensor can also be displayed by the brightness of the LED bulb. When we put the temperature sensor in liquid nitrogen at room temperature (Figure 7D), we

https://doi.org/10.1021/acssuschemeng.1c07174
ACS Sustainable Chem. Eng. 2022, 10, 1847−1856

can find that the brightness of the LED bulb is dimmed (Figure 7E); when the sensor is taken out of the liquid nitrogen and gradually returned to room temperature, the bulb will brighten again (Figure 7F), indicating that the sensor can withstand ultralow temperature.

The Ink/Glue/NR sensor used for temperature detection can also be reflected in the temperature change caused by light irradiation. Herein, we use xenon lamp light to simulate sunlight. Figure S8A shows the detection process of light. The surface temperature of the sensor can be changed by placing the sensor in the xenon light source. When the light source shines on the surface of the sensor, the temperature of the sensor gradually rises, and it has been verified that the resistance of the sensor decreases when the temperature rises. Figure S8B,C,D shows resistance changes of the multifunctional sensors when we put the sensor under xenon light and move the sensor away from xenon light. When the sensor is illuminated, the sensor absorbs the energy of the light and raises its own temperature. Previously, it has been confirmed that the resistance of the multifunction sensor is inversely proportional to the temperature, so when the temperature increases, the resistance of the sensor decreases. Similarly, when the sensor is no longer exposed to light, its surface temperature will gradually decrease, and so the resistance increases. As the light intensity increases, the resistance of the sensor changes more. When the sensor is illuminated again because its own temperature will not immediately drop to the initial value, $\Delta R/R_0$ cannot be returned to 0. This leads to a baseline deviation in the $\Delta R/R_0$ versus time curve. As the number of cycles increases, the overall temperature of the sensor is on the rise, so $\Delta R_{max}/R_0$ are gradually decreased.

CONCLUSIONS

Flexible sensors of NR with various detection functions were successfully prepared using dip-coating technology using Chinese ink and PVA glue as raw materials. SEM characterization of the sensor demonstrated that ICN was well coated on the NR surface with high stability with the help of PVA glue. The excellent stability of the sensor allows it to be used to detect various types of human movement, such as large human movements walking and elbow bending, as well as tiny human movements such as breathing and pronunciation. Moreover, the monitoring of temperature, humidity, and pressure by Ink/Glue/NR sensors can be used for special tasks, such as environmental survey, earthquake prevention, and so forth. Ink/Glue/NR sensors developed in this work have the advantages of good stability, low price, and easy functionalization, which provides a platform for the market of human wearable devices. The raw materials of Chinese ink and PVA glue for preparing the sensor are cheap and easy to obtain, which provides a bright prospect for the introduction of flexible wearable devices in the industry.

MATERIALS AND METHODS

Materials. Chinese ink (Zhujiang brand) was purchased from Guangzhou jinjian office manufacturing plant, China. PVA glue (NO. 15) was obtained from Shanghai Double Happiness Co., Ltd. NR latex gloves were purchased from Haimen Yangzi Medical Equipment Co., Ltd., China. Dimethyl silicone oil was purchased from Sinopharm chemical reagent Co., Ltd., China. PBS was purchased from Thermo Fisher Scientific Inc., USA.

Preparation of Ink/Glue Composites. The solid content of raw ink was determined as 11.46 wt.%. The ink was mixed with PVA glue in different mass ratios (ink: glue = 0.5:1, 1:1, 1.5:1, 2:1, and 3:1) and stirred magnetically at 600 rpm for 30 min.

Preparation of Flexible Sensors. The ink/glue mixture was evenly coated on the surface of the NR latex gloves and dried at 60 °C for at least 24 h. During the drying process, the PVA glue gradually solidifies, and the ICN can be adhered to the surface of the gloves. Finally, the glove was cut to the desired rectangular shape with a knife to prepare the Ink/Glue/NR sensor. When the sensor was prepared, the conductivity was tested. If the conductivity of the newly prepared sensor was basically consistent at different regions, it could be considered that the mixture of Chinese ink and glue was uniform.

Characterization of Chinese Ink. 0.05 wt % Chinese ink dispersion was prepared for determination. The morphology of Chinese ink was analyzed by TEM (JEM, 1400 Flash, USA) and SEM (Zeiss Sigma 500, Germany). The XRD pattern was determined by XRD (Rigaku, Miniflflex600, Cu-Kα, Japan) at an accelerating voltage of 40 kV and the current of 40 mA. The XPS machine (Thermo SCIENTIFIC K-Alpha) was performed to analyze elemental distribution and contents of ICN. Raman spectra of the ink dispersion were conducted with a Raman spectrometer (Lab RAM HR Evolution, HORIBA, Japan). The UV−vis spectrum was obtained by a UV−visible spectrophotometer (Evolution 201, Thermo Scientific, USA). The particle size distribution and ζ potential were obtained using a Nano ZS ζ-potential analyzer (Malvern Instruments Co., U.K.).

Electrical Conductivity Determination of Ink/Glue/NR Sensors. The conductivity was measured with a multimeter (Fluke 17B+). The conductivity was calculated according to the following formula:

$$G = \frac{L}{RS} \tag{1}$$

where G is the conductivity (S/m), L is the length of the sample in the energized direction (m), R is the resistance of the sample (Ω), and S is the cross-sectional area of the sample perpendicular to the direction of energization (m^2).

Stability Test of Ink/Glue/NR Sensors. In order to test the long-term stability of the Ink/Glue/NR sensor, the stretch−recovery cycle test was used. The Ink/Glue/NR sensor used here was covered by a composite with a mass ratio of ink to glue of 2:1. First, the Ink/Glue/NR sensor was connected with the electrometer, then the tester holds the fixture of the electrometer and continuously pulls the Ink/Glue/NR sensor by hand, and the amplitude of each stretch remains the same.

The Ink/Glue/NR sensor coated with a composite with a mass ratio of ink and glue of 2:1 was used to measure its initial resistance (R_0). Then, 100, 200, 500, 1000, and 2000 stretch−recovery cycles were performed, and its resistance with a multimeter was measured immediately after the end of each stage of stretch−recovery cycle.

In order to illustrate that the ink/glue composite was a conductor with excellent stability and flexibility, the Ink/Glue/NR sensor was connected with a LED lamp and a power supply. The sensor was bent and folded to observe the brightness of the LED lamp, and the brightness of the bulb was compared when the sensor was standing still.

The sensor was put into three bottles with 1 mol/L HCl, 1 mol/L NaOH, and 0.01 mol/L PBS. The bottles are stored in the dark at 25 °C for 30 days. After 30 days, the sensor was observed to check whether the ink/glue composite still adhered to the NR matrix.

Strain Detection Performance. The Ink/Glue/NR sensor was connected with the electrometer and stretched gently, and the signal response was recorded. Tape was used to stick the wires on the table to minimize the shaking. The response and recovery time of the Ink/Glue/NR sensor was calculated. The pressure sensor performance was also conducted in a similar way. The tester gently pressed the sensor with his different fingers, and the signal response was recorded with an electrometer.

Humidity Monitoring. First, the sensor and the electrometer were connected with electric wires. Whether the sensor responded to changes in humidity was determined by moving the sensor close to

https://doi.org/10.1021/acssuschemeng.1c07174
ACS Sustainable Chem. Eng. 2022, 10, 1847−1856

and away from the humidifier. After confirming that the sensor had a signal response to humidity, humidification efficiency of the humidifier (33.3, 66.7, and 100%) was adjusted to measure the relationship between the resistance response signal of the sensor and the humidity.

Temperature Monitoring. The sensor was attached to the outer wall of the beaker with tape, and a thermometer was put inside the beaker. Dimethyl silicone oil was added to the beaker, and the sensor temperature (10−90 °C) was changed by heating the oil. Sensor, power supply (voltage of 5 V), and an LED lamp were connected in series to constitute a circuit. The sensor was placed at room temperature (25 °C), and the LED lamp was lit; then, the sensor was placed in liquid nitrogen to observe the brightness of the LED lamp. Then, the sensor was removed from the liquid nitrogen, and the brightness of the LED lamp changed and was observed by placing it at room temperature.

■ ASSOCIATED CONTENT

Supporting Information

The Supporting Information is available free of charge at https://pubs.acs.org/doi/10.1021/acssuschemeng.1c07174.

Basic characterization of Chinese ink, XPS result of ICN, stability of Ink/Glue/NR sensors in different environments, resistance changes of Ink/Glue/NR sensors upon pressure by different fingers, detection of resistance signal change when mobile phone plays at different volumes, detection of ruler vibration by the Ink/Glue/NR sensors, detection of human facial expression, detection of temperature changes caused by light irradiation, comparison of the performance, and price between Chinese ink and other carbon materials (PDF)

■ AUTHOR INFORMATION

Corresponding Author

Mingxian Liu − *Department of Materials Science and Engineering, Jinan University, Guangzhou 510632, China;* orcid.org/0000-0002-5466-3024; Email: liumx@jnu.edu.cn

Authors

Banghan Liu − *Department of Materials Science and Engineering, Jinan University, Guangzhou 510632, China*

Youquan Zhou − *Department of Materials Science and Engineering, Jinan University, Guangzhou 510632, China*

Linhong Chen − *Department of Materials Science and Engineering, Jinan University, Guangzhou 510632, China*

Yue Feng − *Department of Materials Science and Engineering, Jinan University, Guangzhou 510632, China*

Complete contact information is available at: https://pubs.acs.org/10.1021/acssuschemeng.1c07174

Author Contributions

Conception and design by B.H.L., Y.Q.Z., L.H.C., Y.F., and M.X.L.; experiments by B.H.L., Y.Q.Z., and L.H.C.; analysis by B.H.L. and Y.F.; writing by B.H.L. and Y.F. with contributions from B.H.L., Y.F., L.H.C., and M.X.L.; review and editing by B.H.L., Y.Q.Z., L.H.C., Y.F., and M.X.L.; supervision by M.X.L; and funding acquisition by M.X.L.

Notes

The authors declare no competing financial interest.

■ ACKNOWLEDGMENTS

Funding: This work was financially supported by National Natural Science Foundation of China (52073121), Natural Science Foundation of Guangdong Province (2019A1515011509), Science and Technology Planning Project of Guangzhou (202102010117), and the Fundamental Research Funds for the Central Universities (21619102).

■ REFERENCES

(1) Han, S. T.; Peng, H.; Sun, Q.; Venkatesh, S.; Chung, K. S.; Lau, S. C.; Zhou, Y.; Roy, V. An overview of the development of flexible sensors. *Adv. Mater.* **2017**, *29*, No. 1700375.

(2) Ma, J.; Wu, S.; Cheng, H.; Yang, X.; Wang, S.; Lu, P. Sensitivity-enhanced temperature sensor based on encapsulated S-taper fiber Modal interferometer. *Opt. Laser Technol.* **2021**, *139*, No. 106933.

(3) Zhang, Y.; Cao, Y.; Zhao, Y.; Wang, X.; Ran, S.; Cao, L.; Zhang, L.; Chen, B. Optical temperature sensor based on upconversion luminescence of Er^{3+} doped $GdTaO_4$ phosphors. *J. Am. Ceram. Soc.* **2021**, *104*, 361−368.

(4) Ren, X.; Gao, J.; Shi, H.; Huang, L.; Zhao, S.; Xu, S. A highly sensitive all-fiber temperature sensor based on the enhanced green upconversion luminescence in Lu_2MoO_6: Er^{3+}/Yb^{3+} phosphors by co-doping Li^+ ions. *Optik* **2021**, *227*, No. 166084.

(5) Zhu, P.; Kuang, Y.; Wei, Y.; Li, F.; Ou, H.; Jiang, F.; Chen, G. Electrostatic self-assembly enabled flexible paper-based humidity sensor with high sensitivity and superior durability. *Chem. Eng. J.* **2021**, *404*, No. 127105.

(6) Duan, Z.; Jiang, Y.; Zhao, Q.; Huang, Q.; Wang, S.; Zhang, Y.; Wu, Y.; Liu, B.; Zhen, Y.; Tai, H. Daily writing carbon ink: Novel application on humidity sensor with wide detection range, low detection limit and high detection resolution. *Sens. Actuators, B* **2021**, *339*, No. 129884.

(7) Owji, E.; Mokhtari, H.; Ostovari, F.; Darazereshki, B.; Shakiba, N. 2D materials coated on etched optical fibers as humidity sensor. *Sci. Rep.* **2021**, *11*, 1771.

(8) Yao, D.; Wu, L.; Peng, S.; Gao, X.; Lu, C.; Yu, Z.; Wang, X.; Li, C.; He, Y. Use of Surface Penetration Technology to Fabricate Superhydrophobic Multifunctional Strain Sensors with an Ultrawide Sensing Range. *ACS Appl. Mater. Interfaces* **2021**, *13*, 11284−11295.

(9) Cheng, B.; Wu, P. Scalable Fabrication of Kevlar/$Ti_3C_2T_x$ MXene Intelligent Wearable Fabrics with Multiple Sensory Capabilities. *ACS Nano* **2021**, *15*, 8676−8685.

(10) Wang, X.-M.; Tao, L.-Q.; Yuan, M.; Wang, Z.-P.; Yu, J.; Xie, D.; Luo, F.; Chen, X.; Wong, C. Sea urchin-like microstructure pressure sensors with an ultra-broad range and high sensitivity. *Nat. Commun.* **2021**, *12*, 1776.

(11) Wu, Z.; Ai, J.; Huang, J.; Du, Z.; Su, B. A ball-in-ball type self-powered magnetoelectric inertial sensor for 3D multi-angle motion monitoring of humanoid robots. *Nano Energy* **2021**, *85*, No. 106016.

(12) Zhang, X.; Ai, J.; Zou, R.; Su, B. Compressible and Stretchable Magnetoelectric Sensors Based on Liquid Metals for Highly Sensitive, Self-Powered Respiratory Monitoring. *ACS Appl. Mater. Interfaces* **2021**, *13*, 15727−15737.

(13) Ma, Z.; Ai, J.; Shi, Y.; Wang, K.; Su, B. A Superhydrophobic Droplet-Based Magnetoelectric Hybrid System to Generate Electricity and Collect Water Simultaneously. *Adv. Mater.* **2020**, *32*, No. 2006839.

(14) Zhang, P.; Guo, W.; Guo, Z. H.; Ma, Y.; Gao, L.; Cong, Z.; Zhao, X. J.; Qiao, L.; Pu, X.; Wang, Z. L. Dynamically Crosslinked Dry Ion-Conducting Elastomers for Soft Iontronics. *Adv. Mater.* **2021**, *33*, No. e2101396.

(15) Bu, Y.; Shen, T.; Yang, W.; Yang, S.; Zhao, Y.; Liu, H.; Zheng, Y.; Liu, C.; Shen, C. Ultrasensitive strain sensor based on superhydrophobic microcracked conductive $Ti_3C_2T_x$ MXene/paper for human-motion monitoring and E-skin. *Sci. Bull.* **2021**, *66*, 1849−1857.

(16) Wang, H.; Li, J.; Yu, X.; Yan, G.; Tang, X.; Sun, Y.; Zeng, X.; Lin, L. Cellulose nanocrystalline hydrogel based on a choline chloride

deep eutectic solvent as wearable strain sensor for human motion. *Carbohydr. Polym.* **2021**, *255*, No. 117443.
(17) Chu, Z.; Jiao, W.; Huang, Y.; Zheng, Y.; Wang, R.; He, X. Superhydrophobic gradient wrinkle strain sensor with ultra-high sensitivity and broad strain range for motion monitoring. *J. Mater. Chem. A* **2021**, *9*, 9634−9643.
(18) Wang, X.; Liu, X.; Schubert, D. W. Highly sensitive ultrathin flexible thermoplastic polyurethane/carbon black fibrous film strain sensor with adjustable scaffold networks. *Nano-Micro Lett.* **2021**, *13*, 64.
(19) Liu, Y.; Zheng, H.; Liu, M. High performance strain sensors based on chitosan/carbon black composite sponges. *Mater. Des.* **2018**, *141*, 276−285.
(20) Liu, Y.; Wu, F.; Zhao, X.; Liu, M. High-performance strain sensors based on spirally structured composites with carbon black, chitin nanocrystals, and natural rubber. *ACS Sustainable Chem. Eng.* **2018**, *6*, 10595−10605.
(21) Hu, Y.; Zhang, M.; Qin, C.; Qian, X.; Zhang, L.; Zhou, J.; Lu, A. Transparent, conductive cellulose hydrogel for flexible sensor and triboelectric nanogenerator at subzero temperature. *Carbohydr. Polym.* **2021**, *265*, No. 118078.
(22) Li, H.; Zheng, H.; Tan, Y. J.; Tor, S. B.; Zhou, K. Development of an Ultrastretchable Double-Network Hydrogel for Flexible Strain Sensors. *ACS Appl. Mater. Interfaces* **2021**, *13*, 12814−12823.
(23) Zhao, L.; Ren, Z.; Liu, X.; Ling, Q.; Li, Z.; Gu, H. A Multifunctional, Self-Healing, Self-Adhesive, and Conductive Sodium Alginate/Poly (vinyl alcohol) Composite Hydrogel as a Flexible Strain Sensor. *ACS Appl. Mater. Interfaces* **2021**, *13*, 11344−11355.
(24) Zhai, W.; Li, X.; Xia, Q.; Zhan, P.; Xu, J.; Zheng, G.; Dai, K.; Zhang, Z.; Liu, C.; Shen, C. Multi-functional and flexible helical fiber sensor for micro-deformation detection, temperature sensing and ammonia gas monitoring. *Composites, Part B* **2021**, *211*, No. 108621.
(25) Wang, L.; Zhang, M.; Yang, B.; Ding, X.; Tan, J.; Song, S.; Nie, J. Flexible, Robust, and Durable Aramid Fiber/CNT Composite Paper as a Multifunctional Sensor for Wearable Applications. *ACS Appl. Mater. Interfaces* **2021**, *13*, 5486−5497.
(26) Xiong, C.; Xu, J.; Han, Q.; Qin, C.; Dai, L.; Ni, Y. Construction of flexible cellulose nanofiber fiber@ graphene quantum dots hybrid film applied in supercapacitor and sensor. *Cellulose* **2021**, *28*, 10359−10372.
(27) Wang, Y.; Guan, Y.; Liao, D.; He, Y.; Li, S.; Zhou, L.; Yu, C.; Chen, Y.; Liu, Y.; Liu, H. Fabrication of Cellulose Nanofiber/Reduced Graphene Oxide/Nitrile Rubber Flexible Films Using Pickering Emulsion Technology for Electromagnetic Interference Shielding and Piezoresistive Sensor. *Macromol. Mater. Eng.* **2021**, *306*, No. 2100070.
(28) Koivikko, A.; Lampinen, V.; Yiannacou, K.; Sharma, V.; Sariola, V. Biodegradable, Flexible and Transparent Tactile Pressure Sensor Based on Rubber Leaf Skeletons. *IEEE Sens. J.* **2021**, DOI: 10.1109/JSEN.2021.3078807.
(29) Mahmoudpour, M.; Saadati, A.; Hasanzadeh, M.; Kholafazad-kordasht, H. A stretchable glove sensor toward rapid monitoring of trifluralin: A new platform for the on-site recognition of herbicides based on wearable flexible sensor technology using lab-on-glove. *J. Mol. Recognit.* **2021**, *34*, e2923.
(30) Xiao, Y.; Jiang, S.; Li, Y.; Zhang, W. Screen-printed flexible negative temperature coefficient temperature sensor based on polyvinyl chloride/carbon black composites. *Smart Mater. Struct.* **2021**, *30*, No. 025035.
(31) Ji, C.; Zhang, Q.; Jing, Z.; Liu, Y.; Han, D.; Wang, J.; Zhang, W.; Sang, S. Highly Sensitive Wearable Flexible Pressure Sensor Based on Conductive Carbon Black/Sponge. *IEEE Trans. Electron Devices* **2021**, *68*, 5198−5203.
(32) Nag, A.; Alahi, M.; Eshrat, E.; Mukhopadhyay, S. C.; Liu, Z. Multi-Walled Carbon Nanotubes-Based Sensors for Strain Sensing Applications. *Sensors* **2021**, *21*, 1261.
(33) Herren, B.; Webster, V.; Davidson, E.; Saha, M. C.; Altan, M. C.; Liu, Y. PDMS Sponges with Embedded Carbon Nanotubes as Piezoresistive Sensors for Human Motion Detection. *Nanomaterials* **2021**, *11*, 1740.
(34) Sankar, V.; Balasubramaniam, K.; Sundara, R. Insights into the effect of polymer functionalization of multiwalled carbon nanotubes in the design of flexible strain sensor. *Sens. Actuators, A* **2021**, *322*, No. 112605.
(35) Zhu, B.; Niu, Z.; Wang, H.; Leow, W. R.; Wang, H.; Li, Y.; Zheng, L.; Wei, J.; Huo, F.; Chen, X. Microstructured graphene arrays for highly sensitive flexible tactile sensors. *Small* **2014**, *10*, 3625−3631.
(36) Wang, Y.; Yang, R.; Shi, Z.; Zhang, L.; Shi, D.; Wang, E.; Zhang, G. Super-elastic graphene ripples for flexible strain sensors. *ACS Nano* **2011**, *5*, 3645−3650.
(37) Swider, J. R.; Hackley, V. A.; Winter, J. Characterization of Chinese ink in size and surface. *J. Cult. Herit.* **2003**, *4*, 175−186.
(38) Wang, S.; Cao, Y.; Zhang, Q.; Peng, H.; Liang, L.; Li, Q.; Shen, S.; Tuerdi, A.; Xu, Y.; Cai, S. New application of old material: Chinese traditional ink for photothermal therapy of metastatic lymph nodes. *ACS Omega* **2017**, *2*, 5170−5178.
(39) Yang, H. C.; Chen, Z.; Xie, Y.; Wang, J.; Elam, J. W.; Li, W.; Darling, S. B. Chinese ink: A powerful photothermal material for solar steam generation. *Adv. Mater. Interfaces* **2019**, *6*, No. 1801252.
(40) Cao, X.; Liu, H.; Cai, J.; Chen, L.; Yang, X.; Liu, M. Chinese ink coated melamine foam with Joule heating and photothermal effect for strain sensor and seawater desalination. *Composites, Part A* **2021**, *149*, No. 106535.
(41) Jiang, C.; Li, X.; Yao, Y.; Ying, Y.; Ping, J. Fully written flexible potentiometric sensor using two-dimensional nanomaterial-based conductive ink. *Anal. Chem.* **2018**, *90*, 13088−13095.
(42) Liu, H.; Xiang, H.; Wang, Y.; Li, Z.; Qian, L.; Li, P.; Ma, Y.; Zhou, H.; Huang, W. A flexible multimodal sensor that detects strain, humidity, temperature, and pressure with carbon black and reduced graphene oxide hierarchical composite on paper. *ACS Appl. Mater. Interfaces* **2019**, *11*, 40613−40619.
(43) Luo, J.; Gao, S.; Luo, H.; Wang, L.; Huang, X.; Guo, Z.; Lai, X.; Lin, L.; Li, R. K.; Gao, J. Superhydrophobic and breathable smart MXene-based textile for multifunctional wearable sensing electronics. *Chem. Eng. J.* **2021**, *406*, No. 126898.
(44) Bi, P.; Liu, X.; Yang, Y.; Wang, Z.; Shi, J.; Liu, G.; Kong, F.; Zhu, B.; Xiong, R. Silver-Nanoparticle-Modified Polyimide for Multiple Artificial Skin-Sensing Applications. *Adv. Mater. Technol.* **2019**, *4*, No. 1900426.
(45) Liu, Q. C.; Li, L.; Xu, J. J.; Chang, Z. W.; Xu, D.; Yin, Y. B.; Yang, X. Y.; Liu, T.; Jiang, Y. S.; Yan, J. M. Flexible and foldable Li−O_2 battery based on paper-ink cathode. *Adv. Mater.* **2015**, *27*, 8095−8101.
(46) Ferrari, A. C.; Basko, D. M. Raman spectroscopy as a versatile tool for studying the properties of graphene. *Nat. Nanotechnol.* **2013**, *8*, 235−246.
(47) Li, D.; Müller, M. B.; Gilje, S.; Kaner, R. B.; Wallace, G. G. Processable aqueous dispersions of graphene nanosheets. *Nat. Nanotechnol.* **2008**, *3*, 101−105.
(48) Mansur, H. S.; Sadahira, C. M.; Souza, A. N.; Mansur, A. A. FTIR spectroscopy characterization of poly (vinyl alcohol) hydrogel with different hydrolysis degree and chemically crosslinked with glutaraldehyde. *Mater. Sci. Eng., C* **2008**, *28*, 539−548.
(49) Sharma, A.; Kyotani, T.; Tomita, A. Comparison of structural parameters of PF carbon from XRD and HRTEM techniques. *Carbon* **2000**, *38*, 1977−1984.
(50) El-Shamy, A.; Attia, W.; Abd El-Kader, K. The optical and mechanical properties of PVA-Ag nanocomposite films. *J. Alloys Compd.* **2014**, *590*, 309−312.
(51) Bae, S.-H.; Lee, Y.; Sharma, B. K.; Lee, H.-J.; Kim, J.-H.; Ahn, J.-H. Graphene-based transparent strain sensor. *Carbon* **2013**, *51*, 236−242.
(52) Hu, N.; Karube, Y.; Arai, M.; Watanabe, T.; Yan, C.; Li, Y.; Liu, Y.; Fukunaga, H. Investigation on sensitivity of a polymer/carbon nanotube composite strain sensor. *Carbon* **2010**, *48*, 680−687.

Supporting Information

High-performance Sensors Based on Chinese Ink and Water-based Glue for Detection of Strain, Temperature and Humidity

*Banghan Liu, Youquan Zhou, Linhong Chen, Yue Feng, Mingxian Liu**

Department of Materials Science and Engineering, Jinan University, Guangzhou

510632, China

*Corresponding author. Email: liumx@jnu.edu.cn

Number of Pages: 8

Number of Figures: 8

Number of Tables: 1

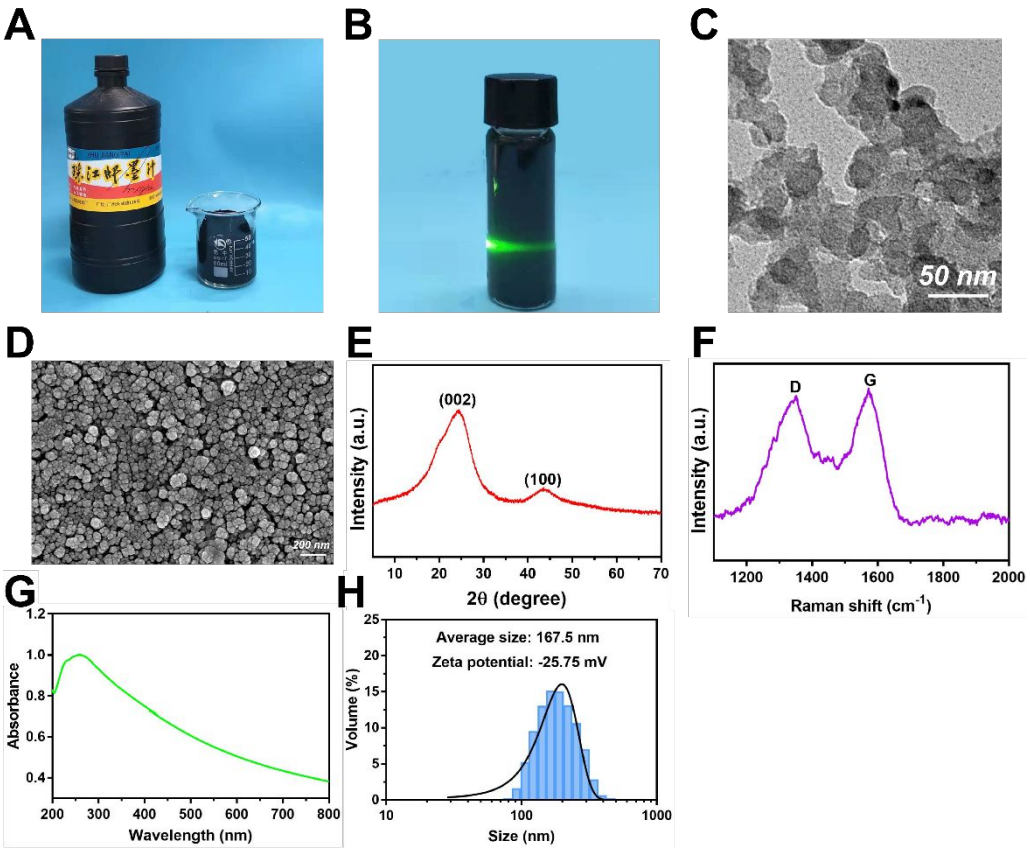

Figure S1. (**A**) The photo of Chinese ink. (**B**) Chinese ink dispersion with a distinct Tyndall scattering effect. (**C**) TEM image of ICN. (**D**) SEM image of ICN. (**E**) The XRD pattern of ICN. (**F**) Raman spectrum of ICN. (**G**) UV-vis spectrum of ICN dispersion. (**H**) Particle size distribution and zeta potential of ICN dispersion.

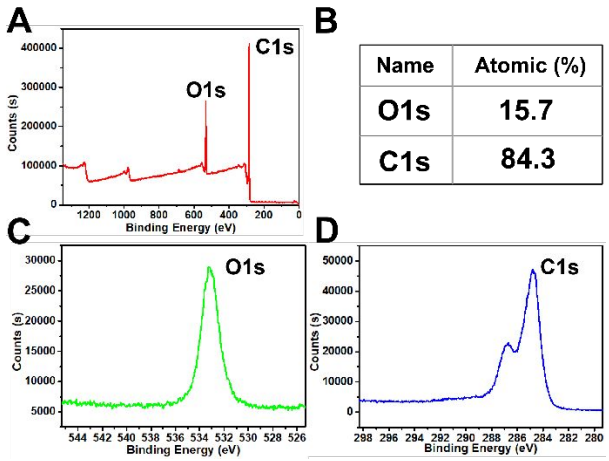

Name	Atomic (%)
O1s	15.7
C1s	84.3

Figure S2. (A) The survey of XPS spectra of ICN. (B) The contents table of ICN. High-resolution curves of (C) O, and (D) C.

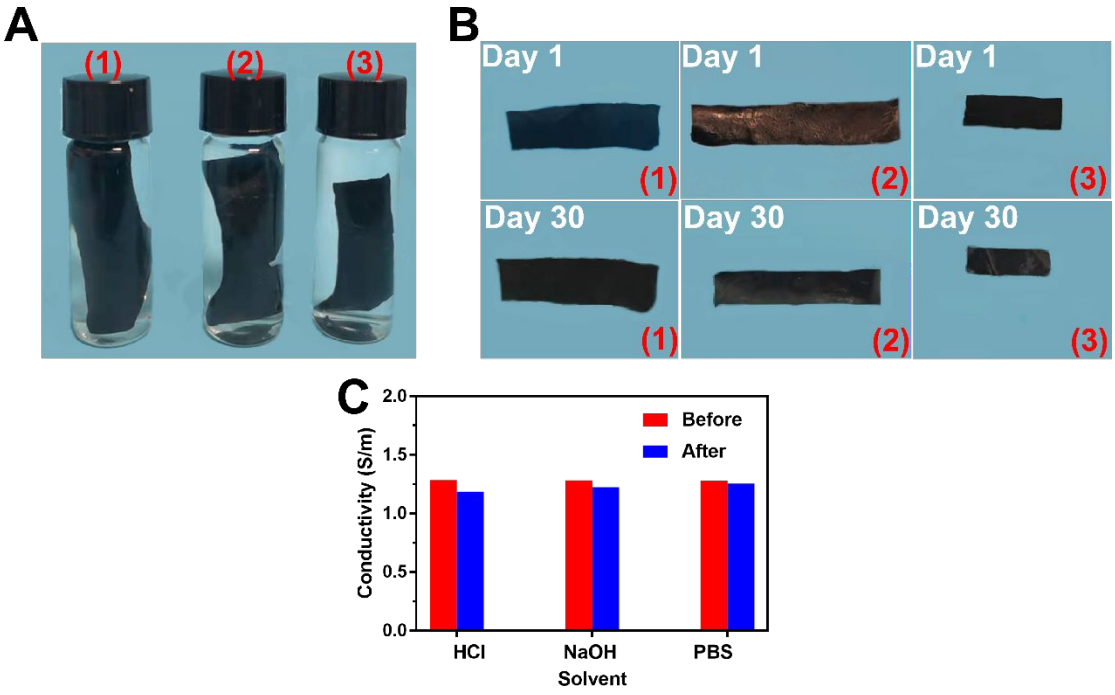

Figure S3. (**A**) Ink/Glue/NR sensors placed in different environments: (1) 1 mol/L HCl; (2) 1 mol/L NaOH; (3) 0.01 mol/L PBS; (**B**) The appearance before and after the Ink/Glue/NR sensors were placed in different environments for 30 days. (**C**) Change of electrical conductivity of Ink/Glue/NR sensor before and after immersing.

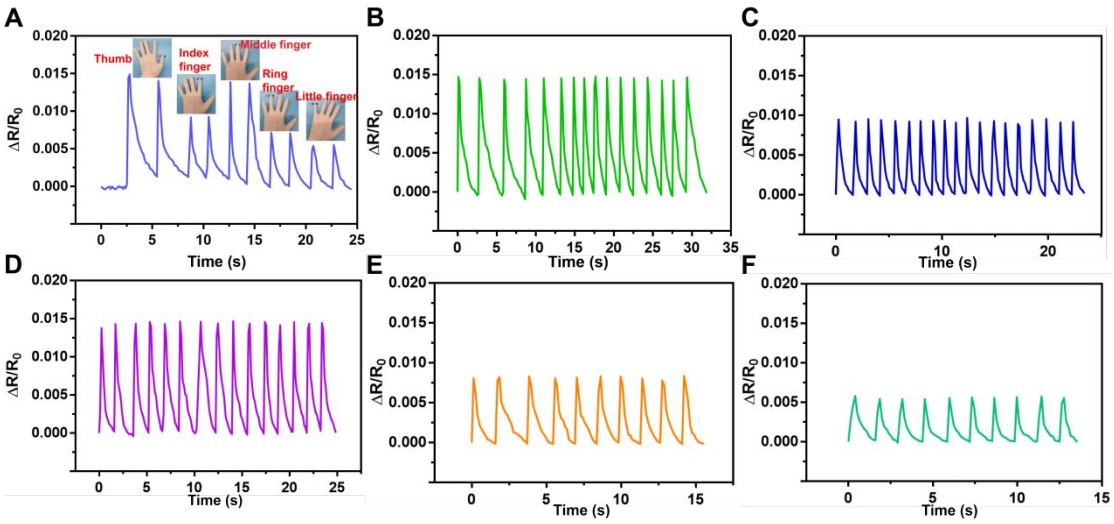

Figure S4. (A) Resistance changes of Ink/Glue/NR sensor upon pressure by different fingers: (B) thumb, (C) index finger, (D) middle finger, (E) ring finger, and (F) little finger.

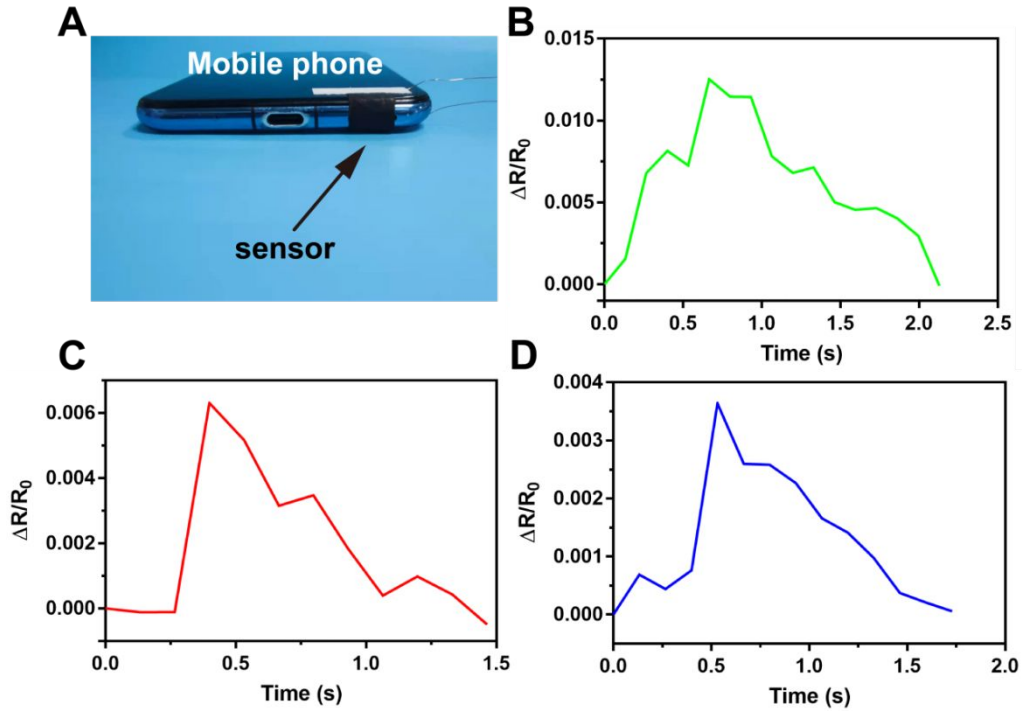

Figure S5. (**A**) The image of the detection process of mobile phone vibration. The resistance signal change when mobile phone plays different volume: (**B**) maximum volume; (**C**) 80% of maximum volume; (**D**) 60% of maximum volume.

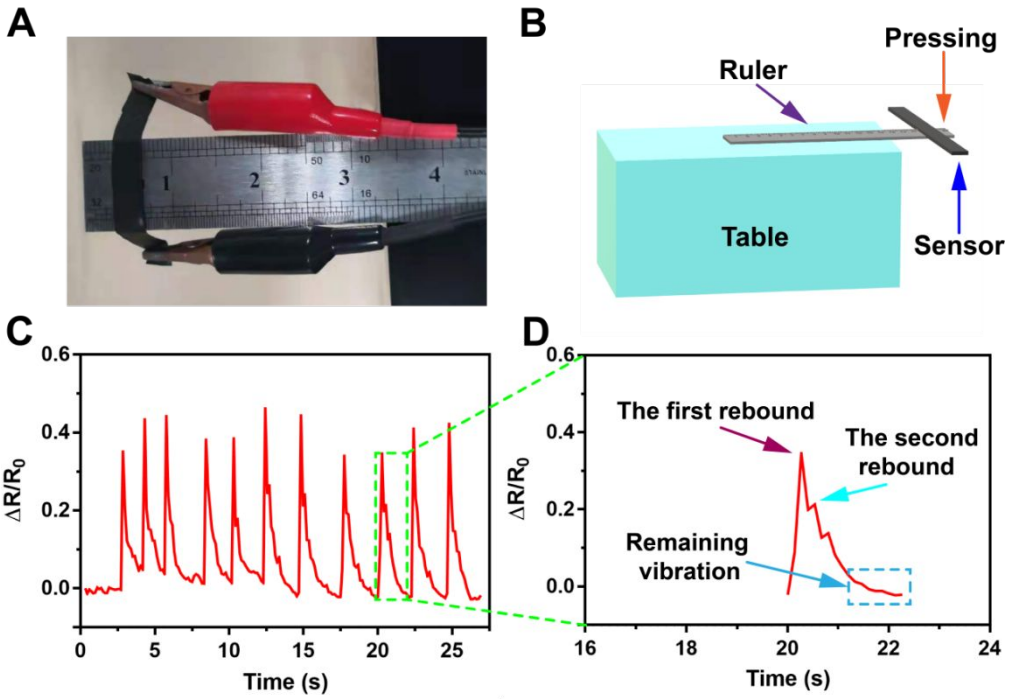

Figure S6. (**A**) Detection of ruler vibration; (**B**) Schematic diagram of vibration detection; (**C**) Resistance changes of multifunctional sensor in the process of ruler vibration; (**D**) One of resistance changes in (**C**).

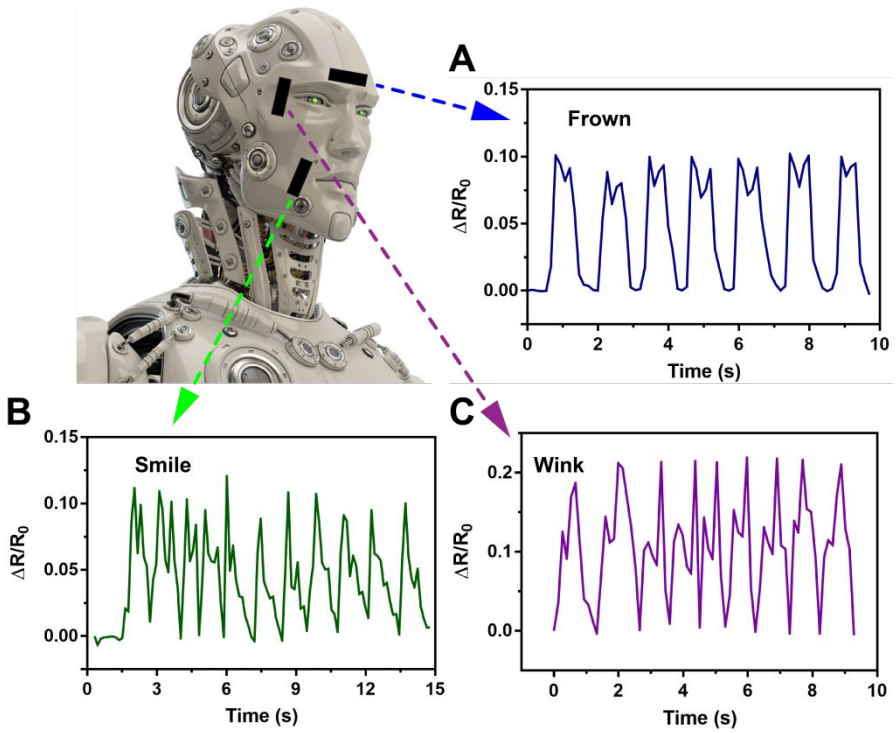

Figure S7. Detection of human facial expression: (A) frown; (B) smile; (C) wink.

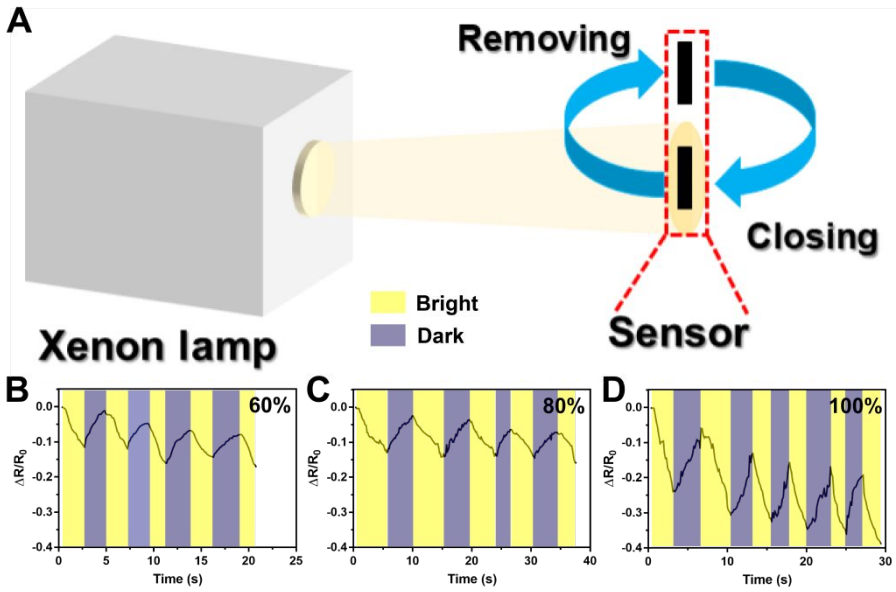

Figure S8. (A) Diagram of an Ink/Glue/NR sensor used to detect temperature changes caused by light irradiation. Resistance changes of Ink/Glue/NR sensors when different light intensity shines on Ink/Glue/NR sensor: (B) 60%; (C) 80%; (D) 100% intensity of xenon lamp.

Table S1. Comparison of the performance and price between Chinese ink and other carbon materials.

Materials	Stretchability	Gauge factor	Response time	Price
Carbon black[1]	1.6%	1.8	340 ms	
Carbon black[2]	10%	2.1	40 ms	$20-25/kg
Carbon black[3]	50%	1.13	-	
Carbon nanotube[4]	700%	3.39	300 ms	$20,000-30,000/kg
Carbon nanotube[5]	74%	58.7	-	
Graphene[6]	300%	25.2	80 ms	$200-2,000/kg
Graphene[7]	-	10.28	112 ms	
Graphene[8]	100%	7.1	-	
ICN	150%	10.2	132.81 ms	$18.4/kg

References

(1) Liu, H.; Xiang, H.; Wang, Y.; Li, Z.; Qian, L.; Li, P.; Ma, Y.; Zhou, H.; Huang, W. A flexible multimodal sensor that detects strain, humidity, temperature, and pressure with carbon black and reduced graphene oxide hierarchical composite on paper. *ACS applied materials & interfaces* **2019,** *11* (43), 40613-40619, DOI: 10.1021/acsami.9b13349.

(2) Liu, P.; Liu, J.; Zhu, X.; Wu, C.; Liu, Y.; Pan, W.; Zhao, J.; Guo, X.; Liu, C.; Huang, Y. A highly adhesive flexible strain sensor based on ultra-violet adhesive filled by graphene and carbon black for wearable monitoring. *Composites Science and Technology* **2019,** *182*, 107771, DOI: 10.1016/j.compscitech.2019.107771.

(3) Xia, Y.; Zhang, Q.; Wu, X. E.; Kirk, T. V.; Chen, X. D. Practical and Durable Flexible Strain Sensors Based on Conductive Carbon Black and Silicone Blends for Large Scale Motion Monitoring Applications. *Sensors* **2019,** *19* (20), 4553, DOI: 10.3390/s19204553.

(4) Sun, X.; Qin, Z.; Ye, L.; Zhang, H.; Yu, Q.; Wu, X.; Li, J.; Yao, F. Carbon nanotubes reinforced hydrogel as flexible strain sensor with high stretchability and mechanically toughness. *Chemical Engineering Journal* **2020,** *382*, 122832, DOI: 10.1016/j.cej.2019.122832.

(5) Min, S.-H.; Lee, G.-Y.; Ahn, S.-H. Direct printing of highly sensitive, stretchable, and durable strain sensor based on silver nanoparticles/multi-walled carbon nanotubes composites. *Composites Part B: Engineering* **2019,** *161*, 395-401, DOI: 10.1016/j.compositesb.2018.12.107.

(6) Liu, C.; Han, S.; Xu, H.; Wu, J.; Liu, C. Multifunctional highly sensitive multiscale stretchable strain sensor based on a graphene/glycerol–KCl synergistic conductive network. *ACS applied materials & interfaces* **2018,** *10* (37), 31716-31724, DOI: 10.1021/acsami.8b12674.

(7) Huang, S.; He, G.; Yang, C.; Wu, J.; Guo, C.; Hang, T.; Li, B.; Yang, C.; Liu, D.; Chen, H.-J. Stretchable strain vector sensor based on parallelly aligned vertical graphene. *ACS applied materials & interfaces* **2018,** *11* (1), 1294-1302, DOI: 10.1021/acsami.8b18210.

(8) Yang, Z.; Pang, Y.; Han, X.-l.; Yang, Y.; Ling, J.; Jian, M.; Zhang, Y.; Yang, Y.; Ren, T.-L. Graphene textile strain sensor with negative resistance variation for human motion detection. *ACS nano* **2018,** *12* (9), 9134-9141, DOI: 10.1021/acsnano.8b03391.